AusRock 2014: Third Australasian Ground Control in Mining Conference

Paper Number: 89

A Strain-Based Failure Criterion for Pillar Stability Analysis

O Gaede[1], C Schrank[2], I Canbulat[3], A Karrech[4]

1.
Lecturer, Science and Engineering Faculty - Queensland University of Technology, GPO Box 2434, Brisbane, QLD, 4001. Email: oliver.gaede@qut.edu.au
Adjunct Research Fellow, School of Earth and Environment - University of Western Australia

2.
Senior Lecturer, Science and Engineering Faculty - Queensland University of Technology, GPO Box 2434, Brisbane, QLD, 4001. Email: christoph.schrank@qut.edu.au
Adjunct Research Fellow, School of Earth and Environment - University of Western Australia

3.
Principal Geotechnical Engineer (Undergrounds), Anglo American Coal, GPO Box 1410, Brisbane Qld 4001. Email: ismet.canbulat@angloamerican.com.au

4.
Associate Professor, School of Civil and Resource Engineering - The University of Western Australia, 35 Stirling Hwy, Crawley WA 6009. Email: ali.karrech@uwa.edu.au

ABSTRACT

Strain-based failure criteria have several advantages over stress-based failure criteria: they can account for elastic and inelastic strains, they utilise direct, observables effects instead of inferred effects (strain gauges vs. stress estimates), and model complete stress-strain curves including pre-peak, non-linear elasticity and post-peak strain weakening. In this study, a strain-based failure criterion derived from thermodynamic first principles utilising the concepts of continuum damage mechanics is presented. Furthermore, implementation of this failure criterion into a finite-element simulation is demonstrated and applied to the stability of underground mining coal pillars.

In numerical studies, pillar strength is usually expressed in terms of critical stresses or stress-based failure criteria where scaling with pillar width and height is common. Previous publications have employed the finite-element method for pillar stability analysis using stress-based failure criterion such as Mohr-Coulomb and Hoek-Brown or stress-based scalar damage models.

A novel constitutive material model, which takes into consideration anisotropy as well as elastic strain and damage as state variables has been developed and is presented in this paper. The damage threshold and its evolution are strain-controlled, and coupling of the state variables is achieved through the damage-induced degradation of the elasticity tensor. This material model is implemented into the finite-element software ABAQUS and can be applied to 3D problems.

Initial results show that this new material model is capable of describing the non-linear behaviour of geomaterials commonly observed before peak strength is reached as well as post-peak strain softening. Furthermore, it is demonstrated that the model can account for directional dependency of failure behaviour (i.e. anisotropy) and has the potential to be expanded to environmental controls like temperature or moisture.

INTRODUCTION

Pillars are load-bearing elements left between underground excavations, which are designed to reduce or control displacements in the near-field domains. They are essential elements in room-and-pillar mining, but they are also used extensively in longwall mining operations.

Depending on the purpose, a pillar is usually loaded uniaxially; however, due to internal and external shear stresses (i.e., at the roof-floor-and-pillar boundaries of excavations), pillars are also loaded biaxially. Nevertheless, a true triaxial stress-state does exist in a pillar and the surrounding rock, as the excavation and pillar act as a stress concentrator and stress rotator.

Pillar performance is controlled by the inherent strength of coal, cleating, fracturing, internal friction angle, cohesion, surrounding strata, the geometry of the pillar (i.e. shape and size) and floor/roof/pillar contact conditions. Insufficient strength can lead to pillar instability and thus collapse of the surrounding rock with potentially catastrophic consequences. Failure mechanism can be controlled, over a period of time, or sudden depending on the stiffness of the pillar and the stiffness of the overburden. The pillar material is often part of the resource that is to be mined, and its design needs to be optimised for maximum resource recovery while minimising instability potential and the associated risks. Understanding of pillar behaviour is

therefore necessary for this optimisation procedure. This paper focuses on the control of intrinsic material parameters and in situ conditions on pillar behaviour. A novel material model is proposed that can describe the rich mechanical response characteristics of soft rocks such as coal and show the numerical implementation into a finite element code.

Laboratory Observations

The literature on mechanical properties of coals is extensive, and only a few examples are given here for the sake of simplicity. Laboratory measurements of mechanical properties usually aim to determine the elastic properties of a specimen and the limits to its elastic behavior (e.g. "yielding", peak strength). When measuring the elastic properties, dynamic and static methods can be used. Dynamic values are based on ultrasonic velocities, while static values are based on the linear part of a stress-strain curve obtained in a deformation experiment. These two values are usually different, due to the different magnitudes in displacements. Strikingly, the majority of elastic measurements, both dynamic and static, show that coal is an anisotropic material. Sazbo (1981) summaries 12 ultrasonic measurements on coal specimens and shows the elastic anisotropy through the existence of three different Poisson's ratios (orthorhombic symmetry). The Poisson's ratios measured perpendicular to the bedding plane and parallel to one of the cleat sets is usually higher, than the Poisson's ratio in the bedding plane. Szwilski (1984) used static measurement on four different coal specimens to determine three distinct Young's moduli with up to a three-fold difference in moduli measured parallel and perpendicular to bedding planes.

One of the difficulties of applying laboratory measurements to in situ size coal pillars is the strong size dependency of the mechanical properties, especially the peak strength. The peak strength of a coal sample reduces with increasing size, as discussed for example by Bieniawski (1968), Hustrulid (1976) and Canbulat (1997). This indicates that laboratory scale does not coincide with the Representative Volume Element (RVE). Nonetheless, laboratory scale experiments (e.g. Pan et al., 2013) and in situ tests (e.g. Bieniawski, 1968) show that coal behaves primarily as an elastic-brittle material. Such materials are characterised by an initial linear elastic response, followed by pre-peak non-linear behaviour and finally rapid post-peak strain weakening.

Classical Approaches to Pillar Performance

In order to predict coal pillar behaviour, both the boundary conditions and the pillar strength have to be determined. The boundary conditions can be expressed in terms of displacement and/or stress. The vertical stress acting on a pillar is easily obtained as a function of overburden density and depth. Various methods are used to calculate the horizontal stresses acting on the pillar. Darling (2011) suggests non-physical estimates using pillar width and height in order to obtain "average pillar stress". Mohan et al. (2001) propose the use of the uniaxial stress equation with thermal expansion as an analytic estimate, as well as 3D finite element models for a numerical estimate. Jaiswal et al. (2009) use a 3D finite element model with displacement boundary conditions at the top of the pillar model. Wang et al. (2011) use a 2D finite element model with a force load at the top and displacement constrain at the base of the model. Furthermore, Wang et al. (2011) consider a scalar damage model of the form, which results in an effective stress acting in the damaged pillar:

$$E = (1 - D) \cdot E_0$$

Where E is the Young's modulus of the damage material, D is the scalar damage variable with a theoretical range of 0 to 1, and E0 is the Young's modulus of the undamaged material.

The pillar strength is usually expressed in terms of critical stresses or stress-based failure criteria and scaling with pillar width and height is common. Darling (2011) discusses critical stress values based on width and height of pillar and provides a compilation of empirical parameters, associated with these critical stress criteria. An earlier review of such failure criteria can be found in Hustrulid (1976).

Various finite-element implementations of stress-based failure criteria and their application to pillar stability have been published in the last decade. Mohan et al. (2001) implemented a linear Mohr-Coulomb criterion with post-peak strain softening into the finite element code FLAC3D. Further, they discussed a non-linear "Sheorey criterion", which they did not directly implement in FLAC3D but via the manipulation of the Mohr-Coulomb parameters. Jaiswal et al. (2009) compared Mohr-Coulomb and Hoek-Brown with non-associated flow rules. Finally, Wang et al. (2011) presented a scalar damage model, which uses the Mohr-Coulomb criterion as the damage threshold.

None of these publications address the dissipative nature of the failure or damage process and the underlying non-equilibrium thermodynamics. This can potentially lead to the systematic overestimation of the elastic energy stored in a pillar and the proposed material / failure model presented herein can account for such dissipative processes.

GOVERNING EQUATIONS

Reversible Material Behaviour

Estimation of material behaviour begins with the development of a material model by considering an elastic-brittle medium, which uses continuum thermodynamics to derive a theoretical framework that allows for fully coupled elastic deformation and irreversible damage evolution (approach pioneered by Lemaitre and Chaboche, 1978). The damage parameter in the continuum damage mechanics (CDM) approach firstly refers to mechanical damage that reduces the load bearing capacity of the body under consideration.

Helmholtz's free energy ψ as a function of the second order tensors for strain ϵ and damage D:

$$\psi = \psi(\epsilon, D)$$

which can be developed in terms of the invariants of the strain and damage tensor

$$\psi(\epsilon, D) = \xi_1 [tr(\varepsilon)]^2 + \xi_2 tr(\varepsilon^2) + \xi_3 tr(\varepsilon) tr(\varepsilon D) + \xi_4 tr(\varepsilon^2 D)$$

The coefficients ξ_i can be identified in terms of the Lame parameters (Gaede et al., 2013). The partial derivatives of the Helmholtz free energy with respect to strain and damage are the Cauchy stress σ of the damaged material and the thermodynamic force Y associated with damage (referred to as Lemaitre damage force):

$$\sigma = \frac{\partial \psi}{\partial \varepsilon} \; ; Y = \frac{\partial \psi}{\partial D}$$

$$Y = \frac{\partial \psi}{\partial D} = -\frac{\lambda}{2} tr(\varepsilon)\varepsilon - \mu\,\varepsilon^2$$

The above equation shows the Lemaitre damage force explicitly, in order to highlight its sole dependence on the elastic strain. This is considered important as the Lemaitre damage force controls both the damage threshold and the damage evolution. Therefore, it is reasonable to refer to the combined damage threshold and evolution laws, as a "strain-based failure criterion".

The second partial derivative of the Helmholtz free energy with respect to strain is the elasticity tensor of the damage material

$$\tilde{a} = \frac{\partial^2 \Psi}{\partial \varepsilon^2} = \lambda\,1 \otimes 1 + 2\mu\,I - \frac{\lambda}{2}\,(1 \otimes D + D \otimes 1) - \mu\,(ID + DI)$$

where $I = 0.5\,(\delta_{ik}\delta_{jl} + \delta_{il}\delta_{jk})$ is the fourth-order identity tensor and the Kronecker delta $\delta_{ij} = 1$ acts as the second-order unity tensor. The form of the undamaged elasticity tensor (D = 0) is known and hence λ and μ can be identified as the Lame parameters of the undamaged solid. Furthermore, an elastic equivalent of a damaged solid, which is initially isotropic and has three orthogonal damage planes, can be calculated.

Irreversible Material Behaviour

In order to derive the law governing the damage evolution, the dissipative nature of damage needs to be considered. The Helmholtz free energy ψ is a function of the external state variables (strain) and the internal state variables (damage), the dissipation Φ is a function of the internal state variables and the thermodynamic fluxes of the internal state variables (i.e., $\frac{dD}{dt}$). The Clausius-Duhem inequality, which can be interpreted as a local form of the second law of thermodynamics, states that the dissipation always has to be non-negative:

$$\Phi = Y : \dot{D} \geq 0$$

where the dissipation is the double contraction of the damage rate tensor and the damage-force tensor. The principle of maximum dissipation (Ziegler, 1977) states that if the dissipation depends on the flux of the internal variables only (e.g., $\Phi = \Phi\,(\dot{D})$) and the flux is prescribed, the actual dissipative force that is realised is the force that maximizes the dissipation Φ

$$\max \Phi\,(\dot{D})$$

with the constraint that signifies the onset of damage evolution, the so-called damage threshold

$$f(Y) \leq 0$$

The Lagrangian of the optimization problem is

$$\mathcal{L} = -Y : \dot{D} + \tilde{\lambda} \cdot f(Y)$$

Below equation optimises Y by finding the extreme point of the Lagrangian

$$\frac{\partial \mathcal{L}}{\partial Y} = 0 \rightarrow \dot{D} = \tilde{\lambda}\frac{\partial f}{\partial Y}$$

where $\tilde{\lambda}$ is a Lagrange multiplier that is yet to be determined. The damage threshold in a way convenient for the subsequent derivation can be calculated as:

$$f(Y) = M_1|Y_1 - Y_{01}| + M_2|Y_2 - Y_{02}| + M_3|Y_3 - Y_{03}|$$

where M is a material parameter and Y_0 is a linear function of the damage parameter $Y_{0i} = \eta_i \cdot D_{ii} + \text{const.}$ with η being a material parameter akin to the hardening parameter of classical plasticity theory. The material behavior of our elastic-brittle medium using the damage threshold can be summarised as:

$$f = 0 \text{ and } df = 0 \Rightarrow \text{damage evolution}$$
$$f = 0 \text{ and } df < 0 \Rightarrow \text{elastic unloading}$$
$$f < 0 \qquad\qquad \Rightarrow \text{elastic behavior}$$

In order to implement the damage evolution into a finite element simulation, the following equation derives an incremental stress-strain relationship for the material behavior after the onset of damage:

$$\sigma = \frac{\partial \Psi}{\partial \varepsilon} \Rightarrow d\sigma = \frac{\partial^2 \Psi}{\partial^2 \varepsilon} : d\varepsilon + \frac{\partial^2 \Psi}{\partial \varepsilon \partial D} : dD$$

For this the total differential of the damage dD and the constraints imposed by the damage threshold f = 0 and df = 0 have to be considered. First, the following equation establishes the total differential of damage threshold f = f (Y (D))

$$df = \frac{\partial f}{\partial Y} : dY + \frac{\partial f}{\partial D} : dD = M : dY + \eta : dD$$

with

$$dD = d\lambda \frac{\partial f}{\partial Y} = d\lambda M$$

where $\tilde{\lambda} = \dot{\lambda}$ and

$$df = M : dY + d\lambda \eta : M = 0$$

the multiplier $d\lambda$ is:

$$d\lambda = -\frac{M : dY}{\eta : M}$$

$d\lambda M$ develops the incremental relationship further as:

$$d\sigma = \frac{\partial^2 \Psi}{\partial \varepsilon^2} : d\varepsilon + d\lambda \frac{\partial^2 \Psi}{\partial \varepsilon \partial D} : M$$

The full derivation of this material model and an application to borehole stability is presented in Gaede et al. (2013). The possibility to extend the model to environmental parameter such as chemical weakening is outlined in Gaede et al. (2011).

Numerical Implementation via Incremental Relationship

The above incremental relationship is implemented into the finite element code ABAQUS via a Fortran user-subroutine. In Figure 1 a stress-strain curve obtained with the fully coupled elastic-damage constitutive law is shown. The stress-strain curve shows the initial linear elastic response, followed by pre-peak non-linear behaviour and finally rapid post-peak strain weakening; the material behaviour that is intended to be

modelled. The onset of non-linear behaviour is induced by the onset of damage evolution (i.e., the damage threshold). Strain weakening is initiated at the damage threshold, but the peak-strength of the material does not coincide with the damage threshold. Therefore, the presented constitutive material model is consistent with laboratory results for various coals (e.g. Pan et al., 2013).

PILLAR MODEL

In order to investigate the difference between a linear elastic and elastic-damage material model, a 2D plane strain model of a coal pillar is considered. The effective model height is 43 m with a roof and floor thickness of 20.0 m and a pillar height of 3 m. The effective model width is 21m with a pillar width of 15m and a roadway width 6m. Hence, a pillar width to height ratio of 5 is considered. The model size is reduced along the symmetry lines of the geometry, halving the width and height of the model. The model is constrained by lateral displacement boundary conditions (ux=0) at the side of the roof column and the vertical symmetry line of the model geometry. A vertical displacement boundary condition (uy=0) is applied at the base of the model, which is horizontal symmetry line of the geometry (i.e. the middle of the pillar). These displacement boundary conditions result in an effective model of periodic parallel pillars. The model is loaded axially with a stress boundary condition of 4.0 MPa, representing an approximate overburden of 160 m.

Quadratic plane-strain elements are used for the solution. The corner between pillar and roof has to be rounded in the model, in order to avoid a singularity in the solution. The Young's modulus of our model material is E = 3.5 GPa. High and low Poisson's ratio case with $\nu = 0.4$ and $\nu = 0.2$, respectively, have been modelled. In this model, it is considered that the roof behaves linearly, whereas for the pillar linear elastic and damageable elastic behaviours are compared. For the elastic-damage behaviour, the stress-strain curve shown in Figure 1 is used. Other combinations of material parameters will be investigated in future studies.

RESULTS

Table 1 shows the maximum horizontal displacement on the pillar surface and Table 2 the maximum von Mises stress in the pillar body, as simple measures for the overall model behaviour. The maximum horizontal displacement is at the base of the model (i.e., at the centre height of the effective pillar), whereas the maximum von Mises stress develops at the corner between roof and pillar and projects obliquely into the pillar body (see Figures 2).

The first-order observation is the significant difference between the high and low Poisson's ratio case in both the maximum horizontal displacement and the maximum von Mises stress. In both cases, the damage threshold is surpassed inside the pillar close to the corner (i.e., in areas with high deviatoric strains or stresses like the von Mises stress). The damage evolution does not propagate far into the pillar, which can be explained by the dissipation of elastic energy through the damage evolution. The purely elastic model shows that the damage threshold would be surpassed in an area larger than in the fully coupled elastic-brittle model.

The onset of damage evolution results in a reduction of the maximum von Mises stress and an increase (order 10 to 15%) in the maximum horizontal surface displacement. The overall change in stress distribution is relatively small. On the other hand, the increase of maximum surface displacement is significant and is

probably in a range that can be measured with in situ instrumentation. Figures 2 and 3 show the von Mises stress and horizontal displacement distribution in the high Poisson's ratio model without damage evolution. Figure 4 shows the increase in horizontal displacement due to damage (in percent of the maximum horizontal displacement value of the elastic case) for the high Poisson's ratio model.

CONCLUSIONS

Influence of Elastic Anisotropy

The fact that the displacements on the pillar surface and the internal pillar stress strongly depend on the Poisson's ratio indicates that the anisotropic nature of coal needs to be taken into consideration in pillar design. This is a positive finding as the orientation of the pillar surface in regard to the coal symmetry planes may be optimised for pillar stability in the planning process. This is particularly true considering that the elastic anisotropy reported by Sazbo (1981) and Szwilski (1984) is significantly higher than the anisotropy considered in the model presented herein.

The presented finite element model is a 2D plane-strain model and needs to be enhanced to a 3D model for further investigations. A 3D model will be capable of simulating the full effect of the elastic anisotropy (general anisotropy instead of Poisson's ratio approximation) and arbitrary orientation of the material symmetry planes. The presented material model can be implemented into a 3D finite element model.

Difference between Elastic and Damage Formulation

For both high and low Poisson's ratios, the damage evolution leads to a dissipation of the elastic energy and an associated reduction in the elastic stresses. As a result, the maximum horizontal displacements at the external pillar ribs are increased (see Figure 4). This indicates that increased surface displacements are not necessarily linked to increased stress build up inside the pillar. This has direct ramification for the use of surface displacement monitoring and its interpretation in regard to the pillar stability. The results suggest that the damage evolution stabilises the pillar to a certain degree, as it dissipates some of the deviatoric strains and stresses associated with slip failure. At the same time, the accumulation of damage makes the pillar material weaker and more susceptible to further damage evolution. Further investigation, especially calibration with in situ data, is necessary to study the impact of damage evolution on the pillar stability. One possible aim is to determine to strain or damage limit that signifies the overall failure of the pillar.

ACKNOWLEDGEMENTS

REFERENCES

Bieniawski, Z. T. (1968). In situ strength and deformation characteristics of coal. *Engineering Geology*, *2*(5), 325-340.

Canbulat, I. (1997). Investigations into the effect of size and width to height ratio on the strength of the laboratory sized coal specimens. MSc Thesis. University of the Witwatersrand, Republic of South Africa.

Darling, P. (Ed.). (2011). *SME mining engineering handbook* (Vol. 1). SME.

Gaede, O., Karrech, A. and Regenauer-Lieb, K. (2011). *Borehole stability analysis in a rock formation with coupled anisotropic damage and chemical weakening*. Proceedings of the GeoProc 2011 conference, Perth, Australia, 6-9 March 2011.

Gaede, O., Karrech, A., and Regenauer-Lieb, K. (2013). *Anisotropic damage mechanics as a novel approach to improve pre-and post-failure borehole stability analysis*. Geophysical Journal International, 193(3), 1095-1109.

Hustrulid, W. A. (1976). A review of coal pillar strength formulas. Rock Mechanics, 8(2), 115-145.

Jaiswal, A. and Shrivastva, B. K. (2009). *Numerical simulation of coal pillar strength*. International Journal of Rock Mechanics and Mining Sciences, 46(4), 779-788.

Lemaitre, J. and Chaboche, J. L. (1978). Phenomenological approach of damage rupture. *Journal de Mécanique Appliquée*, 2(3), 317-365.

Mohan, G., Sheorey, P. R., and Kushwaha, A. (2001). *Numerical estimation of pillar strength in coal mines*. International Journal of Rock Mechanics and Mining Sciences, 38(8), 1185-1192.

Pan, J., Meng, Z., Hou, Q., Ju, Y., and Cao, Y. (2013). *Coal strength and Young's modulus related to coal rank, compressional velocity and maceral composition*. Journal of Structural Geology, 54, 129-135.

Sazbo, T. L. (1981). *A representative Poisson's ratio for coal.* International Journal of Rock Mechanics and Mining Sciences and Geomechanics Abstracts, 18, 531-533.

Szwilski, A. B. (1984). *Determination of the anisotropic Elastic moduli of coal.* International Journal of Rock Mechanics and Mining Sciences & Geomechanics Abstracts, 21(1), 3-12.

Wang, S. Y., Sloan, S. W., Huang, M. L., and Tang, C. A. (2011). *Numerical study of failure mechanism of serial and parallel rock pillars*. Rock mechanics and rock engineering, 44(2), 179-198.

Ziegler, H. (1977). *An Introduction to thermomechanics,* North-Holland series in Applied Mathematics and Mechanics, North-Holland Publishing Co.
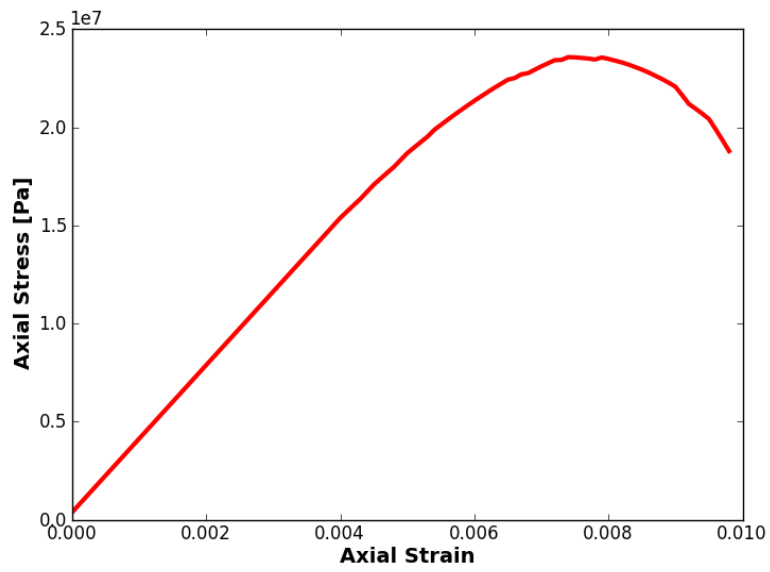
FIGURE CAPTIONS
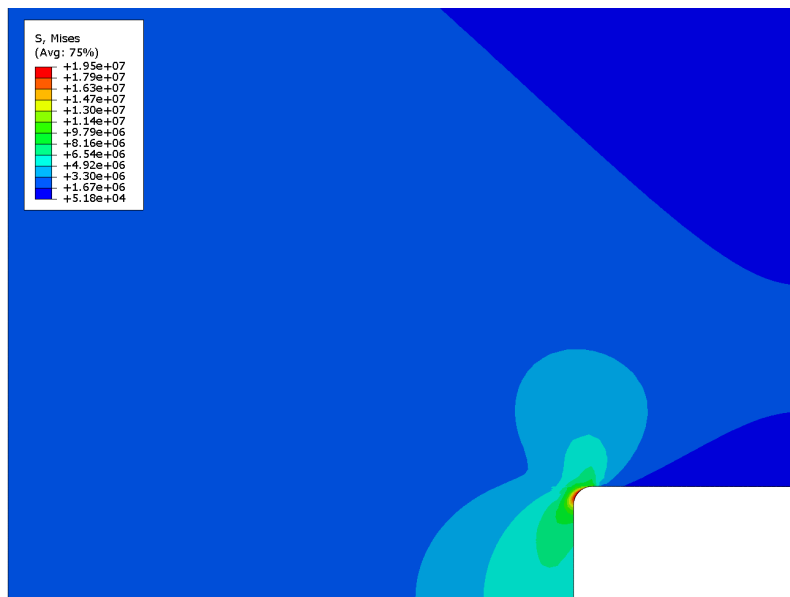
FIG 1 - Stress-Strain curve for fully coupled model

FIG 2 - Von Mises stress distribution without damage evolution; units are in Pa

FIG 3 - Horizontal displacement distribution without damage evolution

FIG 4 - Increase in horizontal displacement due to damage (in %)

TABLE CAPTIONS

TABLE 1

Maximum horizontal displacement on the pillar surface (in m)

TABLE 2

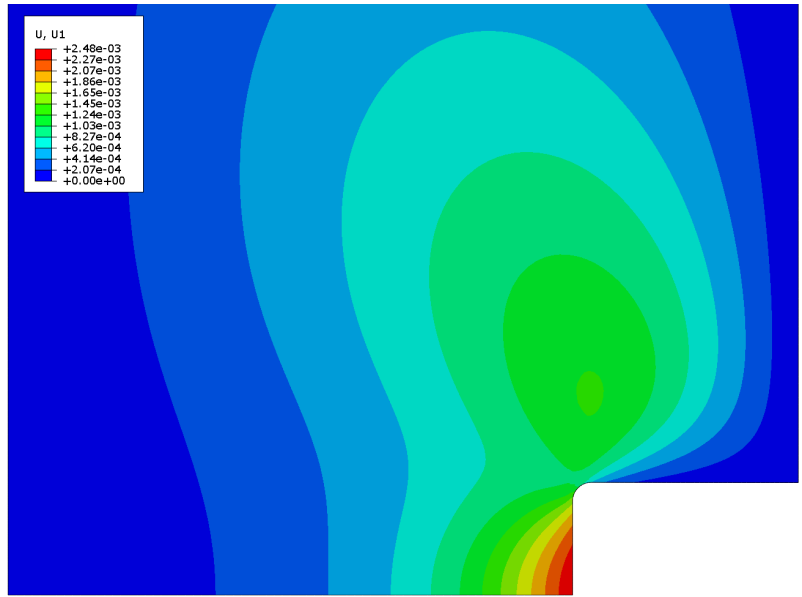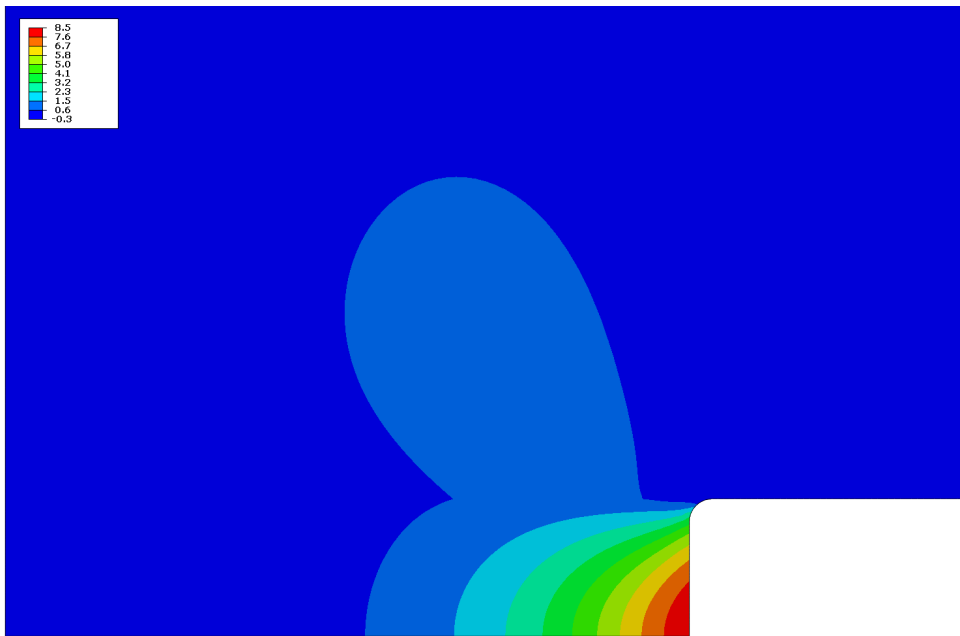Maximum von Mises stress in pillar body (in Pa)

FIGURES

FIG 3 - Horizontal displacement distribution without damage evolution

FIG 4 - Increase in horizontal displacement due to damage (in %)

TABLES

Table 1 Maximum horizontal displacement on the pillar surface (in m)

	High Poisson's Ratio	Low Poisson's Ratio
Elastic Model	2.48×10^{-03}	4.37×10^{-04}
With Damage Evolution	2.71×10^{-03}	5.06×10^{-04}

Table 2 Maximum von Mises stress in pillar body (in Pa)

	High Poisson's Ratio	Low Poisson's Ratio
Elastic Model	1.95×10^{07}	1.92×10^{07}
With Damage Evolution	1.84×10^{07}	1.80×10^{07}